Modulation of the anti-tumor immune response by complement

Maciej M. Markiewski[1], **Robert A. DeAngelis**[1], **Fabian Benencia**[2,3], **Salome K. Ricklin-Lichtsteiner**[1], **Anna Koutoulaki**[1], **Craig Gerard**[4], **George Coukos**[2], and **John D. Lambris**[1]

[1]Department of Pathology and Laboratory Medicine, Medical School of the University of Pennsylvania, 422 Curie Boulevard, Philadelphia, PA 19104

[2]Center for Research on Reproduction and Women's Health, Department of Obstetrics and Gynecology, University of Pennsylvania, 421 Curie Boulevard, Philadelphia, PA 19104

[4]Pulmonary Division, Children's Hospital, Boston, MA 02215, USA

Abstract

The involvement of complement activation products in promoting tumor growth has not yet been recognized. Here we show that generation of complement C5a in the tumor microenvironment enhanced tumor growth by suppressing the anti-tumor CD8^{+} T cell-mediated response. This suppression was associated with the recruitment of myeloid-derived suppressor cells (MDSCs) into tumors and augmentation of their T cell-directed suppressive capabilities. Amplification of MDSC suppressive capacity by C5a occurred through regulation of the production of reactive oxygen and nitrogen species. Pharmacological blockade of C5a receptor significantly impaired tumor growth to a degree comparable to the effect produced by the anti-cancer drug Taxol. Thus, this study demonstrates a therapeutic role for complement inhibition in the treatment of cancer.

Introduction

The diverse roles played by the immune system in cancer initiation and development are illustrated by two concepts: the "cancer immunoediting" theory, which postulates that the immune system protects the host against cancer development[1,2]; and the traditional concept that long-lasting inflammatory reactions facilitate malignant transformation and cancer progression[3–6]. Although an immune reaction develops against malignant tumor cells, tumors have the capacity to suppress this immune response, escaping from immune effector mechanisms[2,7,8]. Antigen-specific CD8^{+} T cell tolerance, induced by myeloid-derived suppressor cells (MDSCs) recruited by tumors, is an example of one such suppression mechanism[9,10]. Although mechanisms responsible for the suppressive phenotype of

MDSCs vary, several studies postulate that MDSCs produce large quantities of reactive oxygen or nitrogen species (ROS or RNS, respectively), which directly inhibit the antigen-specific CD8^{+} T cell-dependent immune response[11]. In addition, L-arginine metabolism regulated by arginase-1 contributes to the generation of these reactive species and seems to have a central role for the suppression of T cells by MDSCs[12]. The immunosuppressive capacity of MDSCs is thought to be one of the major obstacles limiting the use of anti-cancer vaccines[5].

Another potential player in the response to cancer is the complement system, which has an essential role in inflammation and the innate immune response against infections[13]. Complement's wide-ranging activities link the innate immune response to the subsequent activation of adaptive immunity[14]. Circulating complement proteins are activated by limited proteolysis occurring on the surface of pathogens or modified host cells. Some of the resulting cleavage products are deposited on pathogen or host cell surfaces, and others are released into body fluids, where they interact with specific receptors on various target cells. Of these complement components, the C3 protein is considered to be central to the complement cascade. Enzymatic cleavage of C3 leads to the production of the anaphylatoxin C3a, an inflammatory mediator and chemoattractant, and C3b[15]. C3b plays a role in the opsonization and subsequent clearance of pathogens, but is also a main component of the C5 convertase, an enzyme complex that cleaves C5 to produce the anaphylatoxin C5a and C5b. The ensuing cell-surface deposition of the C5b fragment contributes to the formation of the pore-like membrane attack complex (MAC) within cellular membranes, whereas C5a is released and acts as an even more potent chemoattractant and inflammatory mediator than C3a[13,16].

Formation of the MAC leads to the lysis of bacteria or other foreign cells and, under certain pathophysiological conditions, lysis of host cells, as well[13]. Given that several complement components have been found to be deposited in the tumor tissue of patients, the MAC was originally thought to contribute to the immunosurveillance of malignant tumors by complement[17,18]. Further studies revealed, however, that malignant tumor cells are protected against such complement-mediated lysis because they overexpress complement regulators that limit complement activation and deposition *in situ*, and, therefore, the formation of the MAC[17,19]. It has recently been postulated that the ability of the MAC to lyse foreign and host cells might enhance the efficacy of cancer immunotherapies involving monoclonal antibodies specific for particular tumor antigens, since complement proteins enhance antibody-dependent cytotoxicity[20,21].

Despite extensive investigation into the anti-cancer potential of the complement system, a distinctly different role for complement effectors as factors that might promote tumor growth has not yet been explored. Given that complement effectors, such as anaphylatoxins, have strong pro-inflammatory properties[13] and that several inflammatory mediators favor tumor growth[3,5,6], we hypothesized that complement effector proteins might also promote tumor development. Using a syngeneic mouse model of tumor growth[22], we have now shown that various complement deficiencies were associated with impaired tumor enlargement and that pharmacologic blockade of C5a receptor (C5aR) {http://www.signaling-gateway.org/molecule/query?afcsid=A000037} with a peptidic C5aR

antagonist was able to retard tumor growth. Importantly, this inhibition of C5aR signaling was associated with a significantly enhanced CD8^{+} T cell anti-tumor response. The increased immune response was also associated with inhibition of MDSC recruitment into tumors of mice lacking C5aR signaling. In addition, MDSCs isolated from mice deficient in C5aR had a lower capability to inhibit T cell proliferation *in vitro*. The decreased capacity of C5aR-deficient MDSCs to inhibit the antigen-specific CD8^{+} T cell-mediated immune response was associated with the lower production of ROS and RNS by these cells. Thus, our studies demonstrate a role for the complement anaphylatoxin C5a in promoting the growth of malignant tumors through the recruitment of MDSCs into tumors and regulating their functional capacity. These findings point to a new and potentially promising therapeutic application of complement inhibition to the treatment of malignant tumors.

Results

C3 fragments are deposited in engrafted tumors

Many of the functions of complement are mediated by complement effectors such as C3a, C5a and MAC that are generated during the process of complement activation. We hypothesized that these complement effectors are similarly generated during tumor development. In order to test this hypothesis, we used the TC-1 syngeneic model of cervical cancer in mice. In this model, flank tumors rapidly develop after subcutaneous (s.c.) injection of cancer cells. We monitored the activation of complement in these tumor-engrafted mice by immunofluorescent staining, which showed that C3 cleavage products were extensively deposited along the tumor vasculature in wild-type mice (Fig. 1a). As expected, staining was not observed in tumors from C3-deficient mice (data not shown), whereas in benign tissue surrounding tumors in wild-type mice only scattered C3 deposits were visible (Fig. 1b). C3 is the main protein of the complement activation cascade, at which most of the currently known pathways of complement activation converge23. Therefore, the cleavage of C3, as demonstrated by the presence of its cleavage products in tumor tissue, suggests that the activation of complement proteins had occurred in these tumor-bearing mice and had led to the generation of complement effectors. Given that, using available assays, we saw no substantial increase in the concentrations of circulating C3 cleavage fragments in the plasma of these mice (data not shown). These data point to a local and limited activation of complement in the tumor microenvironment rather than systemic complement activation, highlighting the specificity of this phenomenon for tumors.

C3 deficiency inhibits tumor growth

Because the formation of C3 convertase is the point in the complement cascade at which the three known pathways of complement activation converge, the elimination of C3 prevents the generation of complement effectors13; similarly, C3 deficiency eliminates a wide range of activities that are mediated by these effectors. Since we had detected the deposition of C3 cleavage products in the microenvironment of TC-1 tumors, we assessed tumor growth in C3-deficient mice and their littermate controls after subcutaneous (s.c.) inoculation with TC-1 tumor cells. These experiments showed that tumor growth was significantly impaired in the absence of C3 (Fig. 1c). Tumor volumes measured at various times after s.c. inoculation of tumor cells were significantly lower in the C3-deficient mice than in wild-

type littermate controls over the course of the experiment. The absence of the deposition of C3 cleavage products in tumor tissue from C3-deficient mice demonstrated that the injected TC-1 cells were not producing C3 to reconstitute this deficiency. In addition, we monitored the concentrations of C3 in the sera of C3-deficient and control mice throughout the experiment. None of the C3-deficient mice showed detectable concentrations of C3 in their sera, nor was there an increase in the amount of C3 in the wild-type control mice, as determined by ELISA (data not shown). Thus, the impairment of tumor growth in mice lacking C3 strongly suggests that complement and complement activation are intimately involved in this process.

Complement activation pathways in tumors

To elucidate the mechanisms of complement activation (classical, lectin and/or alternative pathways) in TC-1 tumors, we assessed tumor growth in mice deficient in complement protein C4 or complement factor B (fB), as well as their littermate controls, after s.c. inoculation with TC-1 tumor cells. C4 deficiency resulted in greatly reduced tumor growth (Fig. 2a). Given that C4 is required for the formation of the classical or lectin pathway C3 convertases, these results suggest the contribution of one of these pathways to complement activation and subsequent C3 cleavage in engrafted tumors. Deficiency of fB had no substantial effect on tumor growth (Fig. 2b), ruling out any major contribution of the alternative pathway, since fB is an essential component of the alternative pathway C3 convertase.

To dissect whether the classical or lectin pathway is involved in complement activation in tumor tissue, we evaluated TC-1 tumors from wild-type mice for the deposition of complement proteins which initiate these pathways. We found moderate complement protein C1q deposits along tumor vasculature (Fig. 2c), whereas mannan binding lectin (MBL) deposition did not have clear association with tumor blood vessels (Fig. 2d). Since C1q initiates the classical pathway of complement activation and C1q deposition followed the pattern characteristic for C3 deposits, we concluded that this pathway is the main contributor to complement activation in engrafted tumors. The functional relevance of the lectin pathway for complement activation in engrafted tumors remains to be established.

Inhibition of the C5a receptor impairs tumor growth

The C5a anaphylatoxin activates several cellular responses that are involved in tumor growth and progression, including the expression of adhesion molecules on endothelial cells and the release of various cytokines from leukocytes24. These properties of C5a and the results obtained from our study of C3-deficient mice prompted us to investigate whether C5a is required for tumor growth in our model. For this purpose, we blocked the C5a receptor (C5aR) in tumor-bearing wild-type mice with the hexapeptide AcF[OPdChaWR] (C5aR antagonist)25, beginning treatment one week after tumor cell injection.

The pharmacological blockade of the C5aR with this antagonist resulted in impaired tumor growth in the antagonist-treated mice when compared to control mice treated with PBS (Fig. 3a). To estimate whether the therapeutic effectiveness of the C5aR antagonist in retarding tumor growth was comparable to the effects achieved by the treatment of tumor bearing

mice with broadly used anti-cancer drugs, tumor volumes were also assessed in wild-type mice treated with the established anti-cancer drug paclitaxel (Taxol) alone, at a dose previously shown to suppress tumor growth[26]. A comparison between the tumor volumes in the mice treated with the C5aR antagonist and those treated with Taxol showed that inhibition of tumor growth by the complement inhibitor was comparable to that achieved by treatment with this anti-cancer therapeutic (Fig. 3a).

We further verified the specificity of our findings by assessing tumor growth in mice deficient in the C5aR. Consistent with our hypothesis and the results seen in the C5aR antagonist-treated mice, these C5aR-deficient mice exhibited significantly decreased tumor volumes when compared to their littermate controls (Fig. 3b). Further, we found that the suppressive effect of genetic C5aR deficiency on tumor growth was similar to that obtained by treating wild-type mice with Taxol, indicating that lack of the C5aR inhibits tumor growth as well as an established anti-cancer drug (Fig. 3c). These experiments also suggested that C5aR expressed on host cells is involved in the regulation of tumor growth. We initially observed that C5aR mRNA was not present in TC-1 cells under culture conditions (Fig. 3d), but we could not exclude the possibility that C5aR is upregulated in tumor cells *in vivo*. However, if C5aR signaling on TC-1 cells contributed to tumor growth, these cells should still grow in C5aR-deficient mice, as only the host cells lack the ability to express C5aR in these mice. Therefore, these experiments suggest that C5a contributes to the control of tumor growth by acting primarily on receptors expressed by host cells, irrespective of their expression on tumor cells.

To exclude the possibility that that the effect of the C5aR antagonist on tumor growth was related to non-specific cytotoxicity of this peptide toward tumor cells, we evaluated whether the treatment of C5aR-deficient mice with C5aR antagonist further delayed tumor growth. In addition, we also used the peptide-AcF[OPdChaA(d)R] (control peptide), which has the same length and similar physicochemical properties as C5aR antagonist but does not have the ability to block C5aR signaling[25,27]. Use of this control peptide was meant to verify whether alteration of the cellular microenvironment by injected peptides, rather than their biological activity, influences the rate of tumor growth.

The treatment of C5aR-deficient mice did not induce any further inhibition of tumor growth in comparison to mice treated with control peptide (Supplementary Fig. 1 online). In addition, TC-1 tumors grew slower in C5aR-deficient mice in comparison to wild-type controls, as observed in previous experiments, regardless of the treatment of both cohorts with the control peptide (Supplementary Fig. 1). Therefore, we concluded that the effects of the C5aR antagonist on tumor growth in wild-type mice are exclusively related to the property of this peptide to disable C5aR function.

C5a regulates the immune response against tumors

To elucidate the mechanism by which C5a contributes to tumor growth, we assessed several parameters that influence tumor development (tumor cell proliferation and apoptosis, and the extent of angiogenesis) in end-point tumor specimens harvested from mice treated with either C5aR antagonist or PBS. There were only minimal differences between experimental groups in these parameters without statistical significance (Supplementary Fig. 2 online).

This result suggests that other mechanisms, such as tumor cell elimination by the immune system, may contribute to the phenotype observed in mice in which C5a activity was blocked. Given the crucial role of cytotoxic T cells in controlling tumor growth, we next compared the absolute number of CD8$^+$ cells infiltrating the tumor tissue in C5aR antagonist-treated and control mice. Immunofluorescent staining revealed that mice in which C5aR signaling was blocked had tumors heavily infiltrated by CD8$^+$ cells, whereas in a majority of the control mice only a few of these T cells were present in whole-tumor sections (Fig. 4a). Furthermore, quantification of the CD8$^+$ infiltrates showed that there was also an inverse correlation between tumor size and the number of infiltrating CD8$^+$ cells (Fig. 4b).

These data were corroborated by our observation that the percentages of activated CD3$^+$CD8$^+$(CD4$^-$)CD25$^+$ and CD3$^+$CD8$^+$(CD4$^-$)CD69$^+$ T cells were slightly higher in tumors from C5aR-deficient mice than in those from their littermates (n = 3), as estimated by flow cytometry (28.7 ± 3.4% vs. 21.1 ± 1.8% for CD25$^+$ and 24.4 ± 3.2% vs. 16.7 ± 2.2% for CD69$^+$, respectively). However, these differences did not reach statistical significance. Finally, we observed that the size of the white pulp follicles in the spleen was increased, and the proliferation of lymphoid cells residing in these structures was higher in C5aR-deficient mice bearing tumors than in their tumor-bearing littermate controls (Fig. 4c,d).

These results suggested that C5a modulates the CD8$^+$ T cell mediated anti-tumor immune response. Therefore, we hypothesized that slower tumor growth in C5aR-deficient mice and in wild-type mice treated with C5aR antagonist is a result of the infiltration of these tumors by CD8$^+$ T cells. To verify this hypothesis we conducted experiments in which CD8$^+$ T cells were depleted by treatment with CD8-specific antibody in C5aR-deficient and control mice inoculated with tumors cells, expecting that this depletion of CD8$^+$ T cells in C5aR-deficient mice should result in an increased rate of tumor growth. Indeed, even the partial elimination of these cells from C5aR-deficient mice resulted in accelerated tumor growth in these mice to the rate observed in wild-type controls (Fig. 4e). CD8$^+$ T cell depletion did not affect tumor growth in wild-type controls. This result was also expected, based on the observation that only a few CD8$^+$ T cells infiltrated tumors in untreated wild-type mice (Fig. 4a). Preliminary experiments in mice not bearing tumors showed that injections of CD8 antibody at a dose selected to deplete CD8$^+$ T cells resulted in more than 95% depletion of CD8$^+$ T cells (data not shown). However, the monitoring of peripheral blood and spleen of mice bearing tumors revealed that by injecting CD8 antibody we achieved only partial depletion of CD8$^+$ T cells in these mice (Supplementary Fig. 3a,b online), Importantly, though, the degree of CD8$^+$ T cell depletion strongly and positively correlated with the rate of tumor growth in C5aR-deficient mice (Supplementary Fig. 3c,d). This positive correlation confirms that the acceleration of tumor growth in C5aR-deficient mice that had been injected with CD8 antibody was a result of CD8$^+$ T cell depletion. Furthermore, tumors from C5aR-deficient mice treated with CD8 antibody had a lower number of CD8$^+$ T cells than tumors from C5aR-deficient mice treated with control rat IgG, as demonstrated by immunofluorescence analysis (Supplementary Fig. 3e).

C5a regulates the accumulation and migration of MDSCs

Our observations suggested that C5a signaling contributes to the inhibition of the immune response against tumor cells. Cells of myeloid origin, including MDSCs and tumor-associated macrophages (TAMs), have been shown to be important for suppression of the immune response against tumor antigens and promotion of tumor growth in mice and humans. In addition, it is well known that granulocytes, monocytes, and tissue macrophages, which are the mature counterparts of MDSCs, express abundant C5aR[16]. Moreover, we have shown that complement proteins were deposited in tumor tissue (Fig. 1a), suggesting the occurrence of local complement activation, with the concomitant generation of C5a. Therefore, we hypothesized that C5a might contribute to the inhibitory properties of MDSCs.

Our initial studies showed that $CD45^+CD11b^+Gr-1^+$ MDSCs, isolated from the spleen and blood of naive mice, expressed C5aR to a similar extent as that observed in mature granulocytes and monocytes (Supplementary Fig. 4a,b online). Similarly, we observed C5aR expression on the surface of MDSCs circulating in the peripheral blood (Fig. 5a) or residing in the spleen (Fig. 5b) of tumor-bearing mice. The expression of C5aR was reduced on the surface of tumor-associated MDSCs (Fig. 5c) in comparison to peripheral blood and spleen MDSCs. Surprisingly, MDSCs isolated from the tumors of some wild-type mice did not show any surface expression of C5aR (Fig. 5d). However, when MDSCs from the same tumors were permeabilized before staining, C5aR was clearly detectable in the cytoplasm (Fig. 5e). This result demonstrated that C5aR was internalized in tumor associated MDSCs. The rapid internalization of a majority of G-coupled receptors occurs as a regulatory mechanism in response to the constant presence of ligands.

Since C5a is known as a strong chemoattractant[16], we investigated the involvement of C5a in the migration of myeloid-origin cells into tumors. Immunofluorescent staining of tumor sections showed that the number of cells expressing CD11b was lower in C5aR antagonist-treated mice than in mice treated with PBS (Fig. 5f). Interestingly, $CD11b^+$ cells in C5aR antagonist-treated mice were located only at the periphery of the tumors, whereas in control mice they were found throughout the tumor sections. We also saw a positive correlation between the number of $CD11b^+$ cells and the tumor volume in both experimental groups (Fig. 5g).

Flow cytometry analysis of $CD45^+CD11b^+Gr-1^+$ cells isolated from tumors from C5aR-deficient and control mice revealed the presence of two distinct subpopulations of MDSCs differing by the extent of expression of CD11b and Gr-1 (Fig. 5h). These subpopulations corresponded to mononuclear (MO)- and polymorphonuclear (PMN)-MDSCs, which were recently described[28]. PMN-MDSCs were characterized by higher expression of both CD11b and Gr-1 (R1 in Fig. 5h) in comparison to MO-MDSCs (R2 in Fig. 5h). Although the percentage of total MDSCs isolated from tumors from wild-type mice was higher than the percentage of these cells in tumors from C5aR-deficient mice, this difference did not reach statistical significance (Fig. 5i). However, we observed that the ratio of PMN-MDSCs to MO-MDSCs was significantly higher in tumors from wild-type mice in comparison to tumors from C5aR-deficient mice (Fig. 5j). Therefore, we concluded that C5a influences mainly the migration of PMN-MDSCs into tumors. In addition, the percentage of

CD11b^{+}Gr-1^{+} MDSCs in the CD45^{+} cell population isolated from the spleens of wild-type mice was higher than the percentage of these cells existing in the spleens of C5aR-deficient mice (Fig. 5k). This observation suggests the involvement of C5a in the processes of MDSC migration and accumulation into peripheral lymphoid organs.

The migration of PMN-MDSCs to tumors requires crossing of the endothelial barrier by MDSCs. Leukocytes, in order to leave the circulation and migrate to interstitial tissues, require the interaction of their integrins with adhesion molecules on endothelial cells. We hypothesized that the same mechanisms apply to MDSCs migrating to tumor tissue. Since CD11b is the α_M subunit of integrin CR3, which interacts with ICAM-1 expressed on endothelial cells during leukocyte extravasation, we evaluated the changes in CD11b expression in MDSCs obtained from tumors and spleens after C5a stimulation *in vitro*. Wild-type PMN-MDSCs isolated from spleens and tumors showed significant increase in the expression of CD11b after C5a stimulation (Fig. 6a,b), whereas MO-MDSCs did not respond to C5a stimulation by upregulating CD11b (Fig. 6c,d) agreeing with our previous findings showing that C5a stimulates CD11b expression in neutrophils[29]. These results strongly support our hypothesis that C5a contributes to the recruitment of PMN-MDSCs to tumors. The specificity of these findings was confirmed by the lack of CD11b upregulation in C5aR-deficient MDSCs stimulated with C5a (Fig. 6a–d), despite the response of these cells to phorbol myristate acetate (PMA) (Fig. 6 a,b,d), which was used as a positive control to determine the capability of MDSCs to respond to *in vitro* stimuli.

C5a modulates ROS and RNS production in MDSCs

We next analyzed the capacity of Gr-1^{+} MDSCs isolated from tumors obtained from C5aR-deficient and sufficient mice to inhibit the proliferation of CD3^{+} T cells originating from the spleens of naive mice. MDSCs recovered from the tumor microenvironment of C5aR-deficient mice showed either a total inability or a weaker capacity to inhibit phytohemagglutinin (PHA)-induced T cell proliferation than did MDSCs from tumors of littermate controls (Fig. 7a). These observations suggest that C5a contributes not only to the migration of MDSCs into tumors but also to their functional capacity to inhibit the T cell response against tumor cells.

Given that MDSCs are known to inhibit the anti-tumor antigen-specific CD8^{+} T cell response by producing large amounts of highly suppressive ROS and RNS[11], and that C5a is involved in the regulation of ROS and RNS synthesis in macrophages[30] and neutrophils[31], which are thought to be mature counterparts of MDSCs, we hypothesized that C5a influences the suppressive ability of MDSCs through the regulation of their ROS and RNS production. As demonstrated by flow cytometry analysis, the overall amount of ROS and RNS in MDSCs isolated from tumors from C5aR-deficient mice was strikingly lower in comparison to the amounts detected in MDSCs from tumors from wild-type controls (Fig. 7b,c). Since we had observed that C5a influenced the ratio of MO-MDSCs to PMN-MDSCs (Fig. 5j), we analyzed the contribution of both subpopulations to ROS and RNS production. We observed that in both C5aR-deficient and sufficient mice, tumor-associated PMN-MDSCs produced significantly higher amounts of ROS and RNS than corresponding MO-MDSCs (Fig. 7d). However, when comparing the specific subpopulation of PMN-MDSCs

between C5aR-deficient and sufficient mice, we did not see a difference in ROS or RNS production (Fig. 7d). Conversely, MO-MDSCs from tumors growing in C5aR-deficient mice synthesized less ROS and RNS than their wild-type counterparts (Fig. 7d). Therefore, it appears that C5a augments ROS and RNS production only in MO-MDSCs. However, considering that C5a increases the migration of ROS- and RNS-rich PMN-MDSCs into the tumor, high amounts of ROS and RNS in the tumor microenvironment of wild-type mice is a net effect of dual C5a activity. C5a induces the migration of highly suppressive, ROS- and RNS-rich PMN-MDSCs into the tumor microenvironment; additionally, it increases the production of ROS and RNS by MO-MDSCs.

Arginase-1 activity is essential for the immunosuppressive capabilities of MDSCs and contributes to the production of ROS and RNS by these cells[12]. Therefore, we analyzed the expression of this enzyme in available whole-cell extracts from tumors harvested from mice treated with C5aR antagonist or control mice (Fig. 7e). Arginase-1 expression was only slightly lower in mice treated with C5aR antagonist without reaching statistical difference (Fig 7f). However, we observed a strong significant positive correlation between arginase-1 expression and tumor volume (Fig. 7g) in both groups with the correlation coefficient (Pearson r) equal to 0.802.

To further verify the results obtained from these *in vivo* studies, we stimulated MDSCs from spleens and tumors of wild-type mice to produce ROS and RNS by incubating them with various concentrations of C5a *in vitro*. MDSCs isolated from C5aR-deficient mice were used as an additional control for these experiments. Both subpopulations of MDSCs isolated from spleens responded to C5a stimulation by increasing their ROS and RNS production in comparison to non-stimulated cells obtained from the same mouse (Fig. 7h,i). As expected, MDSCs from spleens of C5aR-deficient mice did not respond to C5a stimulation, despite the brisk response to PMA stimulation (Fig. 7h,i). Tumor-associated MDSCs did not respond to C5a stimulation, regardless of which subpopulation of MDSCs was analyzed (data not shown). We concluded that the unresponsiveness of tumor-associated MDSCs to *in vitro* C5a stimulation was a result of the strong stimulation of these cells for ROS and RNS production *in vivo* in the tumor microenvironment and the exhaustion of this system; therefore, further stimulation of these cells *in vitro* failed. This conclusion was supported by the substantially higher initial ROS and RNS production in tumor-associated MDSCs in comparison to MDSCs obtained from spleens (data not shown) and the lack of an increase in ROS or RNS production in tumor-associated MDSCs in response to PMA stimulation (data not shown).

Discussion

Interest in complement as a potential anti-cancer effector system has recently been revived in the context of anti-cancer therapies utilizing monoclonal antibodies raised against tumor cell antigens. Several studies have indicated that blocking or overriding complement regulatory proteins might substantially improve the efficacy of anti-cancer monoclonal antibody immunotherapy[20]. However, despite the large number of studies dedicated to assessing the contribution of complement to cancer pathogenesis and therapy, none of these investigations has addressed a possible role for the complement effectors in promoting the

growth of malignant tumors. This gap in our understanding of the role of complement in cancer is surprising, given that complement effectors, in particular C5a, are potent pro-inflammatory mediators and that inflammation and infections are widely understood to be capable of both promoting and exacerbating tumor growth. The only recent study investigating whether C3 promotes tumor formation involved the development of dyplastic intraepithelial lesions in a model of multistage epithelial carcinogenesis (HPV16 mice). However, that study showed that the activation of complement did not contribute to the recruitment of inflammatory cells, the induction of keratinocyte hyperproliferation, or the activation of angiogenesis during the development of epidermal dysplasia32. The direct comparison of those results with our data is difficult since the model used in this investigation tested the contribution of complement exclusively in pre-malignant skin lesions, whereas we have studied the role of complement in advanced, invasive tumors.

The results of the present study suggest that the complement system indeed contributes to mechanisms that promote the growth of malignant tumors. Utilizing a mouse model of tumor growth in which TC-1 malignant cells were inoculated s.c. into mice, we have demonstrated that C3, C4 and C5aR deficiencies are associated with a retardation of tumor growth. In addition, the pharmacological blockade of the C5aR with a peptidic C5aR antagonist also reduced tumor growth. The effects of treatment of wild-type mice with the C5aR antagonist were comparable to those of the anti-cancer drug paclitaxel when administered to mice at one-sixth the lethal dose. Importantly, the dose of paclitaxel used for our studies was several times higher when compared to the therapeutic dose used for cancer patients (20 mg/kg/week vs. 3.3-4.3 mg/kg every 3 weeks for the treatment of ovarian carcinoma, according to the results of clinical studies provided by the manufacturer). Taken together, these experiments suggest that C5aR signaling promotes the growth of TC-1 tumors.

In most cases, the activation of C5 requires prior activation of C3 (ref. 23). However, under specific pathophysiological conditions, C5a can be generated in the absence of C3 (ref. 33). The similar degree of inhibition of tumor growth that we observed in C3-deficient, C5aR-deficient, and C5aR antagonist-treated mice suggests that, in our experimental model, C5 activation requires prior cleavage of C3 through complement activation. Furthermore, the presence of C3 cleavage products in tumor tissue indicated that C5a was generated locally in the tumor microenvironment and subsequently contributed to mechanisms supporting tumor growth. The impairment of tumor growth in C4-deficient mice together with the local deposition of C1q in tumor tissue points to the involvement of classical pathway in the activation of complement activation during tumor development. Also, the reduced growth of tumors in C5aR-deficient mice suggested that C5a-mediated tumor promoting activity was most relevant to host cells, because the lack of C5aR signaling was limited to these cells under our experimental conditions.

The enhanced infiltration of tumors by CD8^{+} T cells that we observed in mice with blocked C5aR activity points to the possibility that C5a has an immunomodulatory role in tumor growth. Several studies utilizing animal experimental models, as well as studies in humans, have demonstrated a crucial role for cytotoxic CD8^{+} T cells in adaptive immunity against tumors2,34,35. Therefore, given that blocking the C5aR enhanced the CD8^{+} T cell response

in the tumor microenvironment in our model, we hypothesize that C5a promotes the growth of TC-1 tumors by suppressing the adaptive immune response against tumor antigens. This conclusion is further supported by the evident abrogation of the effect of C5aR deficiency on the growth of tumors by depleting CD8^{+} T cells in these mice. Although modulation of the adaptive immune response against tumors by complement is an as-yet unexplored area, several recent studies have demonstrated that complement anaphylatoxins regulate adaptive immune responses at many levels[36–39], particularly in models of allergic disorders[40,41]. Importantly, despite its pro-allergic properties in an inflamed environment, C5a regulates tolerance to inhaled antigens within the respiratory tract. C5aR signaling affects the function of pulmonary dendritic cells and regulatory T cells, leading to suppression of the immune response against airborne antigens[40,42,43]. These immunosuppressive functions of C5a in the respiratory tract support our hypothesis that C5a might have similar capabilities in mice bearing tumors.

One of the important mechanisms utilized by malignant tumors to suppress the immune response to tumor antigens is abnormal myelopoiesis and the recruitment of myelomonocytic cells to the tumor site and peripheral lymphoid organs[9,44]. MDSCs, the subset of these cells that is characterized by coexpression of CD11b and Gr-1 in mice, are the immature counterparts of myeloid-derived antigen-presenting cells and peripheral blood monocytes. MDSCs have the capacity to deregulate and/or suppress T cell-dependent tumor cytotoxicity in tumor-bearing mice and in cancer patients[9]. Considering the effects of C5a on antigen-presenting dendritic cells in the lungs and the well-known chemotactic activity of this anaphylatoxin, we hypothesized that the immunosuppressive capability of C5a is associated with C5a-mediated recruitment and/or activation of MDSCs in tumor-bearing mice. Although these cells are also present in mice without tumors, their numbers are low, and they lack immunosuppressive capabilities[9].

Our initial observations indicated that C5aR expression in MDSCs was similar to its expression on peripheral blood monocytes and granulocytes, which are well-known targets for the pro-inflammatory activities of C5a. High C5aR expression on MDSCs further supported our initial hypothesis. Indeed, tumors harvested from mice lacking C5aR signaling showed only a minimal infiltration by CD11b^{+} myeloid-derived cells, which was limited to the periphery of tumors, whereas wild-type controls had a higher number and a widespread distribution of these cells throughout the tumor tissue. Flow cytometry analysis of CD11b^{+}Gr-1^{+} MDSCs isolated from tumors and spleens of C5aR-deficient and control mice inoculated with TC-1 cells confirmed that C5a contributes to the accumulation of MDSCs in peripheral lymphoid organs, as well as to the migration of these cells into tumors. The peripheral localization of myeloid cells in the tumors of mice lacking C5aR signaling might also suggest that the chemotactic activity of C5a contributes to the migration of these cells throughout the tumor tissue. This hypothesis was further supported by the deposition of C3 cleavage products along the tumor vasculature, indicating that complement activation and subsequent generation of C5a occur in tumor tissue, wherever blood vessels are present.

C5a also influenced the functional properties of MDSCs, as demonstrated by the inability of isolated Gr-1^{+} cells from C5aR-deficient tumor-bearing mice to inhibit CD3^{+} T cell proliferation *in vitro*. This observation was corroborated by the decreased proliferation of

lymphoid cells that we observed in the white pulp of the spleens from these mice. These data agree with previous findings that suppression of the T cell immune response to tumor antigens is not limited to the tumor environment but extends to the peripheral lymphoid organs, where immunosuppressive MDSCs are also present and may interact with tumor-specific cytotoxic T cells9.

Flow cytometry analysis of MDSCs isolated from tumors confirmed that C5a contributes to suppression of the anti-tumor T cell response through regulation of the amount of highly suppressive ROS and RNS in the tumor microenvironment. Interestingly, we have found that C5a has a profound influence on two functionally and morphologically distinct subpopulations of MDSCs: MO-MDSCs and PMN-MDSCs, which were recently described28. We observed that C5a contribute to the recruitment into tumors of PMN-MDSCs, which produced much more ROS and RNS than MO-MDSCs. In addition, C5a increases ROS and RNS production in MO-MDSCs. Thus, the high amounts of T cell suppressive ROS and RNS in the tumor microenvironment is a result of both the recruitment of ROS and RNS-rich PMN-MDSCs into tumors and the upregulation of ROS and RNS production in MO-MDSCs by C5a.

In summary, our study points to a previously undefined role for complement in tumor biology. We have shown that complement activation and C5a signaling are required for the efficient recruitment of MDSCs into tumors and for the ability of these myeloid-derived cells to suppress the CD8+ T cell-mediated anti-tumor response. In addition, we have demonstrated that, in our system, inhibition of complement signaling by pharmacological intervention was as efficient as the well-accepted chemotherapeutic, paclitaxel, in hindering the growth of malignant tumors.

It is important to point out that the data presented in this work were obtained from studies utilizing a single experimental model of tumor growth. Considering the enormous diversity of neoplastic diseases and the context-dependent properties of the complement system45, extrapolation of these results to other experimental, as well as clinical, situations should be made carefully. Further studies are necessary to extend these findings into other relevant cancer-related systems, especially in the context of the dual role of inflammation and infections in cancer pathogenesis46. Our findings support the concept that chronic and moderate inflammation promotes tumor growth. However, it has also long been recognized that acute and brisk inflammation can induce tumor regression46.

The findings reported here not only introduce a new complement-mediated mechanism of tumor-dependent immunosuppression but also provide preliminary evidence for the potential usefulness of a therapeutic option, complement inhibition, in anti-cancer therapy. This perspective is particularly attractive because of the relatively small number of side effects reported for complement-directed therapy47,48, as compared to the high toxicity associated with currently used anti-cancer chemotherapeutics. Moreover, given that complement inhibition overrides tumor-dependent immunosuppression, this therapeutic approach may also have promise as a supplement to anti-tumor vaccines.

Methods

In vivo studies and reagents

All mouse experiments were approved by the University of Pennsylvania Institutional Animal Care and Use Committee according to the National Institutes of Health (NIH) guidelines. Mice deficient in complement component C3, C4, factor B and the C5a receptor (C5aR)-deficient mice utilized in our studies have been previously described[49–52]. Mice deficient in C4 and C57BL/6 mice were purchased from The Jackson Laboratory. Mice were backcrossed for at least nine generations onto a C57BL/6 background, and their homozygous wild-type littermates were used as controls. Mice were housed in an animal facility of the University of Pennsylvania, within a barrier, on a 12-h light/dark cycle. Water and standard rodent diet were provided *ad libitum*.

To establish TC-1 tumors, male and female mice 6–16 weeks of age were anesthetized and injected subcutaneously (s.c.) with 1×10^5 TC-1 cells in the right or left rear flank. The tumorigenic TC-1 cell line, described previously[22], was obtained from the American Type Culture Collection (ATCC Number CRL-2785). Beginning about 2 weeks after cell injection, mice were anesthetized, and their tumors were measured with calipers every 2–4 days until the tumor size required sacrificing of the animals. Measurements were taken in two dimensions (length and width) because the depth of the tumor was difficult to assess in live animals. The depth of the tumor was therefore estimated based on the smaller (width) measurement, and the volume of the tumor was calculated using the formula: (length × width × depth) ÷ 2. One hour prior to sacrifice, 5-bromo-2′-deoxyuridine (BrdU; Sigma) was injected intraperitoneally (i.p.) into mice at a single dose of 50 mg/kg for further assessment of tumor or immune cell proliferation. At the time of sacrifice, clinical status was assessed, the mice were anesthetized, blood was harvested from the inferior vena cava (with 50 mM EDTA), and the spleens and tumors were removed. Excised tumors were measured in three dimensions to obtain an accurate volume and then weighed. Tumors and spleens were cut into sections for cell isolation, histologic examination, or freezing.

To achieve a pharmacological blockade of C5aR, C57BL/6J mice were injected s.c. with 1 mg/kg of the cyclic hexapeptide AcF[OPdChaWR] (C5aR antagonist), in ~400 μl of PBS, every 2–3 days beginning 1 week after tumor cell injection (3.3 μmol/kg/week). The C5aR antagonist was synthesized in our laboratory as previously described[25]. This antagonist has been shown to specifically block C5a-mediated effects in various rodent disease models[47,53]. Paclitaxel (Taxol; Mayne Pharma, Inc.) at a dose of 20 mg/kg in 400 μl PBS was injected i.p. into mice once per week (23 μmol/kg/week, $LD_{50} = 128$ mg/kg according to the manufacturer) starting 1 week after tumor cell injection. Control mice in the experiments utilizing C5aR antagonist or Taxol were injected s.c., or i.p., respectively, with ~400 μl PBS alone, or in some cases, s.c. with the cyclic hexapeptide AcF[OPdChaA(d)R][25,27]. The pattern of the administration of this control peptide to mice followed that described for the C5aR antagonist.

To deplete CD8+ T cells, mice were injected i.p. with rat anti-mouse CD8 monoclonal antibody (mAb 53-6.72) at a dose of 200 μg per mouse for 3 consecutive days. To maintain CD8+ T cell depletion, injections were repeated every 2–3 days beginning from day 6. This

regimen of administration resulted in approximately 95% depletion of CD8^{+} T cells from peripheral blood and spleens of mice without tumors, as evaluated by flow cytometry analysis (data not shown). The rat anti-mouse CD8 antibody was purified from ascites produced in nude BALB/c mice (Cocalico Biologicals, Inc.) inoculated with Hybridoma cell line clone 53-6.72 (ATCC), using a standard protocol of ammonium sulfate and caprylic acid precipitations. To ensure endotoxin-free antibody solution, Detoxi-Gel™ Affinity pack™ kit (Thermo Scientific, Pierce) was used for LPS removal.

All compounds used for *in vivo* studies were tested to be LPS free.

Tissue processing, cell isolation and purification

Portions of tumors and spleens were fixed in 10% formalin, frozen in OCT medium at −70 °C or used for cell isolation. Fixed samples were routinely processed for histological evaluation and immunohistochemical staining. Frozen samples were cut with a cryostat into 5-μm thick sections for immunofluorescent staining. Blood samples, after erythrocyte lysis, were analyzed by flow cytometry to assess the expression of surface markers and C5aR by white blood cells. Portions of tumors and spleens were mechanically disaggregated in order to obtain single-cell suspensions. Erythrocytes were removed prior to cell culture or staining by treatment of cell suspensions with 155 mM NH_4Cl, 10 mM $KHCO_3$, and 1 mM EDTA, pH 7.3, for 5 min on ice. Myeloid precursors were selected by means of magnetic sorting as described previously[10]: In brief, single-cell suspensions obtained from the tumors were pre-incubated with anti-mouse CD16/CD32 mAb (2.4G2) from BD Biosciences to block Fcγ receptors. The cells were then incubated with biotinylated anti-mouse Gr-1 (RB6-8C5) from BD Biosciences for 30 min, washed, and incubated with BD IMag Streptavidin Particles Plus (BD Biosciences) for 30 min at 4 °C and separated using an IMagnet (BD Biosciences).

Cell proliferation, apoptosis and angiogenesis

The morphology of tumors and spleens was assessed by light microscopy (Olympus BX 60) of hematoxylin and eosin-stained 5-μm paraffin sections. To assess the number of cells in the S phase of the cell cycle, paraffin sections from tumors and spleens were stained with anti-BrdU. The presence of apoptotic cells in tumor sections was determined by staining for the activated caspase-3 site on cytokeratin 18. Both assays were performed as described previously[54]. The microvascular density of engrafted tumors was evaluated by immunofluorescent staining for CD31 expression on endothelial cells in frozen sections. The bound biotinylated anti-CD31 (MEC 13.3-BD Biosciences) was visualized with a streptavidin-rhodamine complex (BD Biosciences). Fluorescence was evaluated by standard fluorescent microscopy (Olympus BX 60 microscope). BrdU incorporation into tumor cells and the microvascular density of tumors were quantified in 5–10 microscopic fields (400× for BrdU and 100× for microvascular density) with the use of ImageJ image analysis software (NIH, Bethesda, MD), and mean values were calculated. Apoptosis was assessed in a semi-quantitative manner: Scores from 0 to 4 were assigned to sections, depending on the size of the area occupied by apoptotic cells. All analyses were performed in a blinded fashion.

Complement deposition and immune cell infiltration

The deposition of C3 cleavage products in tumor tissue was detected using a rat anti-mouse C3 mAb (clone 2/11), as described previously[55]. This mAb specifically recognizes epitopes of C3 cleavage products (C3b, iC3b and C3c), but not inactive C3. Therefore, the positive reactivity in the tissue is thought to be associated with the activation of the complement cascade and C3 cleavage. C1q and MBL deposition were evaluated with the use of a rat anti-mouse C1q mAb (Abcam, Inc.,) and a polyclonal goat anti-mouse MBL (Santa Cruz Biotechnology, Inc.), respectively. These sections were co-stained with the use of biotinylated anti-mouse CD31 to visualize tumor vasculature. CD8^{+} T cell and myeloid-origin cell infiltrations of tumors were analyzed using anti-mouse CD8 and anti-mouse CD11b, respectively. Isotypic rat IgGs were used as a negative control. Anti-CD31, anti-CD8 and anti-CD11b and isotype controls were purchased from BD Biosciences. Primary antibodies bound in tissue were detected with donkey anti-rat or anti-goat Cy2-conjugated antibodies (The Jackson Laboratory), except for anti-CD31, which was visualized with a streptavidin-rhodamine complex (BD Biosciences). Immunofluorescent staining was performed on frozen, 5-μm-thick sections. For detection of complement deposition, green and red fluorescence images were merged with the use of Spot software (Diagnostic instruments, Inc.). CD8^{+} tumor infiltrates were quantified using ImageJ image analysis software (NIH), positive cells were counted in whole tissue sections and means were calculated. The magnitude of CD11b^{+} infiltrates was assessed in a semi-quantitative manner because of the relatively low numbers of infiltrating cells. Scores from 0 to 5 were assigned to sections, according to the relative intensity of the infiltrates. In addition, the distribution of infiltrating cells was analyzed. All analyses were performed in a blinded fashion.

Fluorescence-activated cell-sorting analyses

Single-cell suspensions were pre-incubated with anti-mouse CD16/CD32 mAb (Fc block, 2.4G2; BD Pharmingen) to block Fcγ receptors, then incubated with primary antibody. Fluorochrome-conjugated mAbs against mouse CD3 (17A2), CD4 (L3T4), CD8 (53-6.7), CD11b (M1/70), CD25 (PC61), CD45 (30-F11), CD69 (H1.2F3) and Gr-1 (RB6-8C5), (all from BD Biosciences) were used according to the manufacturer's instructions. In order to determine C5aR cell-surface expression, cells were sequentially incubated with rabbit polyclonal anti-mouse C5aR (C1150-32, BD Biosciences) or rabbit isotype (BD Pharmingen, 550875) and FITC-conjugated anti-rabbit IgG (F0112, R&D Systems), or with rat anti-mouse C5aR (mAb clone 20/70 Hycult biotechnology b.v., distributor-Cell science Inc.) or rat isotype (BD Pharmingen, 553928) followed by FITC-conjugated anti-rat IgG (Zymed-Invitrogen). For some experiments cells were permeabilized with the use of fixation and perm/wash buffers (BD Biosciences) prior to C5aR staining. Stained cells were subjected to six-color flow cytometry on a FACSCanto flow cytometer (BD Biosciences) using FlowJo software (Tree Star Inc.).

Preparation of CFSE-labeled T cells

In order to obtain cells for proliferation studies, spleens were harvested from naive C57BL/6J mice and mechanically disrupted by passage through 100-μM mesh cups to obtain single-cell suspensions. After lysis of red blood cells, the splenocytes were pooled,

pelleted by centrifugation, and washed twice in serum-free RPMI. Splenocytes were then labeled with 5,6-carboxyfluorescein diacetate succinimidyl ester (CFSE) (Molecular Probes), as follows: Cells were washed with ice-cold PBS, resuspended at 5×10^6 cells/ml in ice-cold PBS, and labeled by diluting the 0.5 mM CFSE stock 1,000-fold into the cell suspension (final concentration, 0.5 μM) and incubating the cells for 10 min at 37 °C. After labeling, fetal calf serum was added to 5% final concentration, and the cells were immediately centrifuged and washed with ice-cold PBS.

Assay for suppression of T cell proliferation

The suppressive effect of MDSCs on T cell proliferation was assessed in co-culture assays: CFSE-labeled splenocytes (1×10^5) were co-cultured with MDSCs (1×10^5) in the presence of 5 μg/ml PHA (Sigma) for 5 days in RPMI 10% FBS at 37 °C in a 5% CO_2 atmosphere. T cell proliferation was determined by flow cytometry. For this purpose, non-adherent cells were recovered from the co-cultures and stained with fluorochrome-labeled anti-mouse CD3 (BD Bioscience) after blocking Fc receptors. Dilution of the CFSE signal in the FITC channel among CD3 gated cells was considered indicative of proliferation. CFSE-labeled splenocytes cultured with PHA in the absence of MDSCs (maximum proliferation, lowest CFSE signal) and equally labeled non-stimulated splenocytes (basal proliferation, highest CFSE signal) were used as controls.

Quantitative real-time PCR analysis

Expression of C5aR was analyzed at the mRNA level by quantitative real-time reverse transcription (RT)-PCR analysis. Total RNA was isolated with TRIzol reagent (Invitrogen), and the High Capacity cDNA Reverse Transcription Kit (Applied Biosystems) was used for reverse transcription of RNA into DNA according to the manufacturer's instructions. The SYBR® Green PCR Master Mix kit (Applied Biosystems) was used for real-time PCR, as described previously[56]. We used the absolute quantification method by generating standard curves for our genes of interest and reference. Each amplification experiment was performed in 96-well optical-grade PCR plates covered with optical tape in the AbiPrism 7700 Sequence Detection System (Applied Biosystems). The following primers were used: Forward, 5′-CGCTCCACCAAGACGCTCAA-3′; Reverse, 5′-GGGGCAGCCACGCTATCATC-3′. The cDNA load was normalized to mouse glyceraldehyde-3-phosphate dehydrogenase (GAPDH), with primers GAPDH Forward, 5′-CCTGCACCACCAACTGCTTA-3′ and GAPDH Reverse, 5′-CATGAGTCCTTCCACGATACCA-3′. Data were expressed as relative units, normalized to those for 10^4 GAPDH mRNA molecules. Molecules were considered to be present if more than five copies of mRNA were detected for every 10^4 copies of GAPDH mRNA[57].

Preparation of dendritic cells and macrophages

Bone marrow cells were dispersed by vigorous pipetting and cultured in RPMI-1640 supplemented with penicillin (100 μg/ml), streptomycin (100 U/ml), L-glutamine (2 mM), 2-mercaptoethanol (50 μM; Sigma), and 10% heat-inactivated FBS in the presence of 20 ng/ml of recombinant mouse granulocyte-macrophage colony-stimulating factor (GM-CSF, 315-03, Peprotech Inc.) for 8 days. GM-CSF was replenished on days 3 and 6. In some experiments, maturation was induced by culturing the cells for 2 days in the presence of 10

ng/ml GM-CSF, 20 ng/ml mouse tumor necrosis factor (TNF, 315-01A, Peprotech), and 1 μg/ml bacterial lipopolysaccharide (LPS from *E. coli*, serotype 0111:B4, L2630, Sigma). Mouse peritoneal cells were obtained by washing the peritoneal cavity of C57BL/6J mice with complete medium.

ROS and RNS production

The oxidation sensitive dye 2′-7′-dichloro dihydrofluorescein diacetate (H$_2$DCFDA) (Molecular Probes) was used for the measurement of ROS and RNS production in cells isolated from tumors or spleens. The excised tumors and spleens were mechanically disintegrated to obtain a single-cell suspension. Cells resuspended in DMEM were incubated with 2 μM of dye at 37 °C for 15 min. After washing with PBS, cells were stained for flow cytometry analysis as described above. MDSCs were distinguished from other cells present in the cell suspension as a viable CD45$^+$CD11b$^+$Gr-1$^+$ cell population, and the fluorescence intensity was estimated in the channel suitable for FITC according to the manufacturer's instruction. The amounts of ROS and RNS in cells were proportional to the intensity of fluorescence and were expressed as median fluorescence for gated populations. For some experiments, in addition to incubation with H$_2$DCFDA, freshly isolated cells were simultaneously stimulated by 1, 10 or 100 nM of recombinant mouse C5a expressed as previously described[58] or 1 μM of phorbol myristate acetate (PMA; Sigma-Aldrich). Preliminary experiments have shown that stimulation of cells with 10 nM C5a induced the highest induction of ROS and RNS production.

Immunoblots

Whole-cell extracts were prepared from tumor tissue mechanically disrupted in lysis buffer (20 mM HEPES, pH 7.4, 0.2 mM EDTA, 420 mM NaCl, 1.5 mM MgCl$_2$, 20% glycerol) treated with protease and phosphatase inhibitors (1 mM DTT, 0.1 mM PMSF, 0.1 mM Na$_3$VO$_4$, 1 mM NaF, 1 mM β-glycerophosphate, and 2 μg/ml each of antipain dihydrochloride, aprotinin, bestatin and leupeptin). For each protein sample, 40 μg was electrophoresed on a 12% polyacrylamide gel and transferred to a PVDF membrane. Membranes were incubated overnight at 4 °C with mouse monoclonal arginase I (8C9) antibody (Santa Cruz Biotechnology) or mouse monoclonal β-actin (AC-15) antibody (Abcam). Primary antibody binding was detected using HRP-conjugated anti-mouse antibody (Bio-Rad Laboratories, Inc.) and chemiluminescence (Amersham Pharmacia Biotech, Inc.). Protein loading was normalized according to the abundance of β-actin, with Ponceau S-stained membranes used for verification. Protein expression was quantified by densitometry using ImageQuant software (Molecular Dynamics).

Statistics

The effect of genotype or treatment on tumor growth (Figs. 1-4, Supplementary Fig. 1) was analyzed with two-way analysis of variance (ANOVA) using GraphPad Prism (GraphPad Software, Inc.); the Bonferroni post-test correction was applied to control for the occurrence of false-positives. To evaluate the significance of the correlation between tumor volumes and cell infiltrates (Figs. 4,5, Supplementary Fig. 3) or arginase concentrations (Fig. 7), the Pearson correlation test was applied (GraphPad Prism, GraphPad Software, Inc.). Unpaired

two-tailed Student's *t*-test (Microsoft Excel; Microsoft Corp.,) was used to test the significance of differences in the percentages of MDSCs in tumors and spleens (Fig. 5i-k), for assays of tumor cell proliferation and apoptosis and microvascular density (Supplementary Fig. 2), and for the number of T cells in CD8^{+} T cell-depleted mice (Supplementary Fig. 3). To determine whether induction of CD11b (Fig. 6) or ROS (Fig. 7) over baseline values (set to equal 1) was significant, one sample *t*-test was used (GraphPad Prism, GraphPad Software, Inc.). Wilcoxon signed rank test (GraphPad Prism, GraphPad Software, Inc.) was applied to evaluate the significance of differences in median fluorescence values proportional to ROS/RNS production by MDSCs (Fig. 7). A p value equal to or less than 0.05 was considered significant.

Supplementary Material

Refer to Web version on PubMed Central for supplementary material.

Acknowledgments

References

1. Dunn GP, Bruce AT, Ikeda H, Old LJ, Schreiber RD. Cancer immunoediting: from immunosurveillance to tumor escape. Nat Immunol. 2002; 3:991–998. [PubMed: 12407406]

2. Swann JB, Smyth MJ. Immune surveillance of tumors. J Clin Invest. 2007; 117:1137–1146. [PubMed: 17476343]

3. Coussens LM, Werb Z. Inflammation and cancer. Nature. 2002; 420:860–867. [PubMed: 12490959]

4. Balkwill F, Mantovani A. Inflammation and cancer: back to Virchow? Lancet. 2001; 357:539–545. [PubMed: 11229684]

5. Bhardwaj N. Harnessing the immune system to treat cancer. J Clin Invest. 2007; 117:1130–1136. [PubMed: 17476342]

6. Lin WW, Karin M. A cytokine-mediated link between innate immunity, inflammation, and cancer. J Clin Invest. 2007; 117:1175–1183. [PubMed: 17476347]

7. Blank C, et al. PD-L1/B7H-1 inhibits the effector phase of tumor rejection by T cell receptor (TCR) transgenic CD8+ T cells. Cancer Res. 2004; 64:1140–1145. [PubMed: 14871849]

8. Dong H, et al. Tumor-associated B7-H1 promotes T-cell apoptosis: a potential mechanism of immune evasion. Nat Med. 2002; 8:793–800. [PubMed: 12091876]

9. Sica A, Bronte V. Altered macrophage differentiation and immune dysfunction in tumor development. J Clin Invest. 2007; 117:1155–1166. [PubMed: 17476345]

10. Kusmartsev S, Nagaraj S, Gabrilovich DI. Tumor-associated CD8+ T cell tolerance induced by bone marrow-derived immature myeloid cells. J Immunol. 2005; 175:4583–4592. [PubMed: 16177103]

11. Kusmartsev S, Nefedova Y, Yoder D, Gabrilovich DI. Antigen-specific inhibition of CD8+ T cell response by immature myeloid cells in cancer is mediated by reactive oxygen species. J Immunol. 2004; 172:989–999. [PubMed: 14707072]

12. Marx J. Cancer immunology. Cancer's bulwark against immune attack: MDS cells. Science. 2008; 319:154–156. [PubMed: 18187637]

13. Markiewski MM, Lambris JD. The role of complement in inflammatory diseases from behind the scenes into the spotlight. Am J Pathol. 2007; 171:715–727. [PubMed: 17640961]

14. Carroll MC. The complement system in regulation of adaptive immunity. Nat Immunol. 2004; 5:981–986. [PubMed: 15454921]

15. Sahu A, et al. Structure, functions, and evolution of the third complement component and viral molecular mimicry. Immunologic Research. 1998; 17:109–121. [PubMed: 9479573]

16. Guo RF, Ward PA. Role of C5a in inflammatory responses. Annu Rev Immunol. 2005; 23:821–852. [PubMed: 15771587]

17. Fishelson Z, Donin N, Zell S, Schultz S, Kirschfink M. Obstacles to cancer immunotherapy: expression of membrane complement regulatory proteins (mCRPs) in tumors. Mol Immunol. 2003; 40:109–123. [PubMed: 12914817]

18. Donin N, et al. Complement resistance of human carcinoma cells depends on membrane regulatory proteins, protein kinases and sialic acid. Clin exp Immunol. 2003; 131:254–263. [PubMed: 12562385]

19. Donin N, et al. Complement resistance of human carcinoma cells depends on membrane regulatory proteins, protein kinases and sialic acid. Clin exp Immunol. 2003; 131:254–263. [PubMed: 12562385]

20. Macor P, Tedesco F. Complement as effector system in cancer immunotherapy. Immunol Lett. 2007; 111:6–13. [PubMed: 17572509]

21. Gelderman KA, Tomlinson S, Ross GD, Gorter A. Complement function in mAb-mediated cancer immunotherapy. Trends Immunol. 2004; 25:158–164. [PubMed: 15036044]

22. Lin KY, et al. Treatment of established tumors with a novel vaccine that enhances major histocompatibility class II presentation of tumor antigen. Cancer Res. 1996; 56:21–26. [PubMed: 8548765]

23. Sahu A, Lambris JD. Structure and biology of complement protein C3, a connecting link between innate and acquired immunity. Immunol Rev. 2001; 180:35–48. [PubMed: 11414361]

24. Monk PN, Scola AM, Madala P, Fairlie DP. Function, structure and therapeutic potential of complement C5a receptors. Br J Pharmacol. 2007; 152:429–448. [PubMed: 17603557]

25. Finch AM, et al. Low-molecular-weight peptidic and cyclic antagonists of the receptor for the complement factor C5a. J Med Chem. 1999; 42:1965–1974. [PubMed: 10354404]

26. Holtz DO, et al. Should tumor VEGF expression influence decisions on combining low-dose chemotherapy with antiangiogenic therapy? Preclinical modeling in ovarian cancer. J Transl Med. 2008; 6:2. [PubMed: 18182107]

27. Johswich K, et al. Ligand specificity of the anaphylatoxin C5L2 receptor and its regulation on myeloid and epithelial cell lines. J Biol Chem. 2006; 281:39088–39095. [PubMed: 17068344]

28. Movahedi K, et al. Identification of discrete tumor-induced myeloid-derived suppressor cell subpopulations with distinct T-cell suppressive activity. Blood. 2008

29. Mollnes TE, et al. Essential role of the C5a receptor in E coli-induced oxidative burst and phagocytosis revealed by a novel lepirudin-based human whole blood model of inflammation. Blood. 2002; 100:1869–1877. [PubMed: 12176911]

30. Daniel DS, et al. The reduced bactericidal function of complement C5-deficient murine macrophages is associated with defects in the synthesis and delivery of reactive oxygen radicals to mycobacterial phagosomes. J Immunol. 2006; 177:4688–4698. [PubMed: 16982908]

31. Guo RF, et al. Neutrophil C5a receptor and the outcome in a rat model of sepsis. FASEB J. 2003; 17:1889–1891. [PubMed: 12897064]

32. de Visser KE, Korets LV, Coussens LM. Early neoplastic progression is complement independent. Neoplasia. 2004; 6:768–776. [PubMed: 15720803]

33. Huber-Lang M, et al. Generation of C5a in the absence of C3: a new complement activation pathway. Nat Med. 2006; 12:682–687. [PubMed: 16715088]

34. Shankaran V, et al. IFNgamma and lymphocytes prevent primary tumour development and shape tumour immunogenicity. Nature. 2001; 410:1107–1111. [PubMed: 11323675]

35. Smyth MJ, et al. Perforin-mediated cytotoxicity is critical for surveillance of spontaneous lymphoma. J Exp Med. 2000; 192:755–760. [PubMed: 10974040]

36. Hawlisch H, Kohl J. Complement and Toll-like receptors: key regulators of adaptive immune responses. Mol Immunol. 2006; 43:13–21. [PubMed: 16019071]

37. Suresh M, et al. Complement component 3 is required for optimal expansion of CD8 T cells during a systemic viral infection. J Immunol. 2003; 170:788–794. [PubMed: 12517942]

38. Kim AH, et al. Complement C5a receptor is essential for the optimal generation of antiviral CD8+ T cell responses. J Immunol. 2004; 173:2524–2529. [PubMed: 15294968]

39. Liu J, et al. The complement inhibitory protein DAF (CD55) suppresses T cell immunity in vivo. J Exp Med. 2005; 201:567–577. [PubMed: 15710649]

40. Kohl J, Wills-Karp M. Complement regulates inhalation tolerance at the dendritic cell/T cell interface. Mol Immunol. 2007; 44:44–56. [PubMed: 16889830]

41. Kohl J, et al. A regulatory role for the C5a anaphylatoxin in type 2 immunity in asthma. J Clin Invest. 2006; 116:783–796. [PubMed: 16511606]

42. Karp CL, et al. Identification of complement factor 5 as a susceptibility locus for experimental allergic asthma. Nat Immunol. 2000; 1:221–226. [PubMed: 10973279]

43. Peng T, et al. Role of C5 in the development of airway inflammation, airway hyperresponsiveness, and ongoing airway response. J Clin Invest. 2005; 115:1590–1600. [PubMed: 15902311]

44. Gallina G, et al. Tumors induce a subset of inflammatory monocytes with immunosuppressive activity on CD8+ T cells. J Clin Invest. 2006; 116:2777–2790. [PubMed: 17016559]

45. Mastellos D, Lambris JD. Complement: more than a 'guard' against invading pathogens? Trends Immunol. 2002; 23:485–491. [PubMed: 12297420]

46. Mantovani A, Romero P, Palucka AK, Marincola FM. Tumour immunity: effector response to tumour and role of the microenvironment. Lancet. 2008; 371:771–783. [PubMed: 18275997]

47. Kohl J. Drug evaluation: the C5a receptor antagonist PMX-53. Curr Opin Mol Ther. 2006; 8:529–538. [PubMed: 17243489]

48. Ricklin D, Lambris JD. Complement-targeted therapeutics. Nat Biotechnol. 2007; 25:1265–1275. [PubMed: 17989689]

49. Circolo A, et al. Genetic disruption of the murine complement C3 promoter region generates deficient mice with extrahepatic expression of C3 mRNA. Immunopharmacology. 1999; 42:135–149. [PubMed: 10408374]

50. Wessels MR, et al. Studies of group B streptococcal infection in mice deficient in complement component C3 or C4 demonstrate an essential role for complement in both innate and acquired immunity. Proc Natl Acad Sci USA. 1995; 92:11490–11494. [PubMed: 8524789]

51. Matsumoto M, et al. Abrogation of the alternative complement pathway by targeted deletion of murine factor B. Proc Natl Acad Sci USA. 1997; 94:8720–8725. [PubMed: 9238044]

52. Hopken UE, Lu B, Gerard NP, Gerard C. The C5a chemoattractant receptor mediates mucosal defence to infection. Nature. 1996; 383:86–89. [PubMed: 8779720]

53. Holland MC, Morikis D, Lambris JD. Synthetic small-molecule complement inhibitors. Curr Opin Investig Drugs. 2004; 5:1164–1173.

54. Markiewski MM, et al. C3a and C3b activation products of the third component of complement (C3) are critical for normal liver recovery after toxic injury. J Immunol. 2004; 173:747–754. [PubMed: 15240660]

55. Mastellos D, et al. Novel monoclonal antibodies against mouse C3: Description of fine specificity and applications to various immunoassays. Mol Immunol. 2004; 40:1213–1221. [PubMed: 15104126]

56. Conejo-Garcia JR, et al. Tumor-infiltrating dendritic cell precursors recruited by a beta-defensin contribute to vasculogenesis under the influence of Vegf-A. Nat Med. 2004; 10:950–958. [PubMed: 15334073]

57. Benencia F, et al. HSV oncolytic therapy upregulates interferon-inducible chemokines and recruits immune effector cells in ovarian cancer. Mol Ther. 2005; 12:789–802. [PubMed: 15925544]

58. Strey CW, et al. The proinflammatory mediators C3a and C5a are essential for liver regeneration. J Exp Med. 2003; 198:913–923. [PubMed: 12975457]
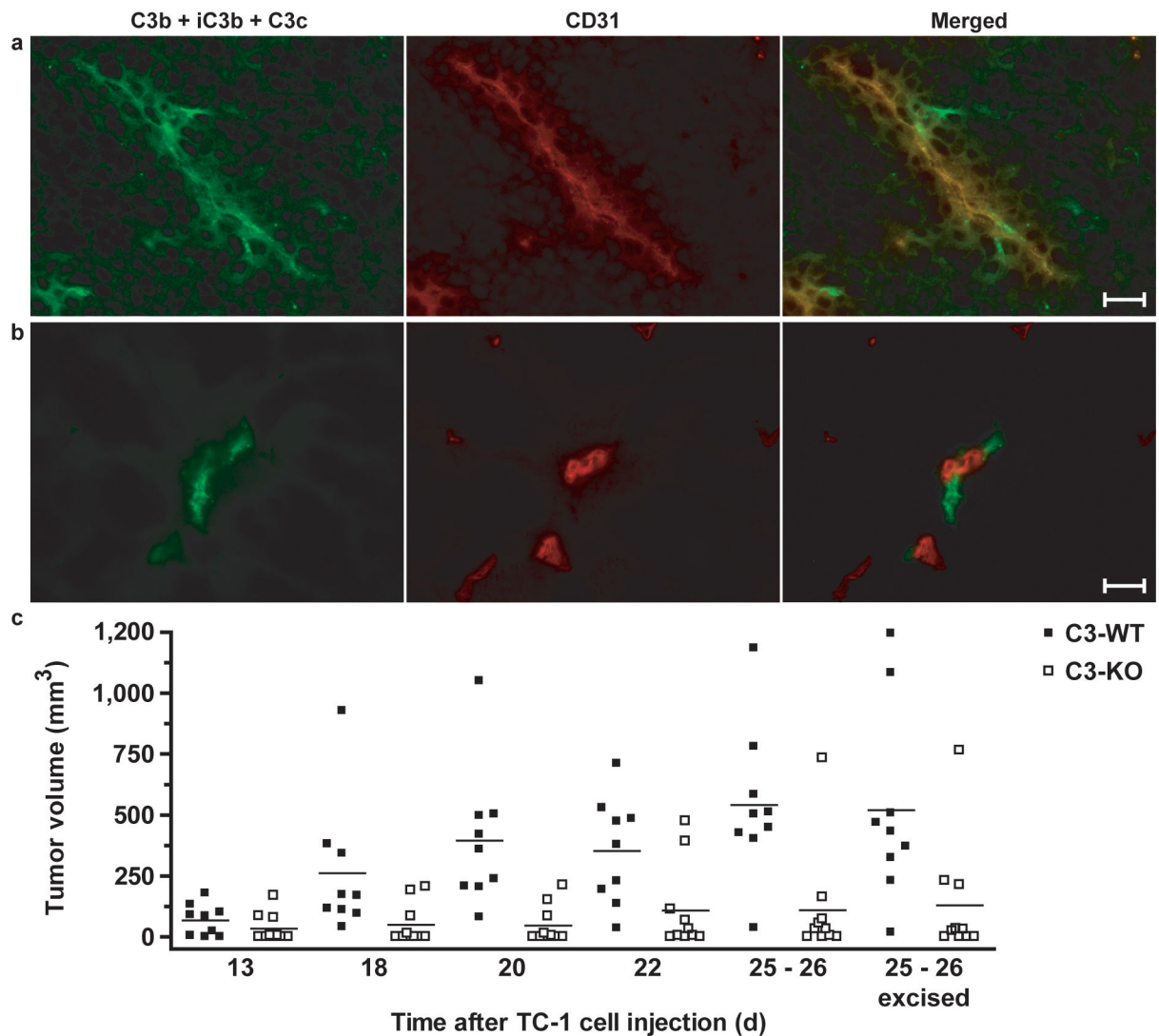
Figure 1.
Complement activation plays a role in tumor growth. **(a, b)** Immunofluorescent detection of complement cleavage products using C3 antibody (left, green fluorescence) or endothelial cells using CD31 antibody (middle, red fluorescence) in frozen sections from a wild-type mouse in an end-point tumor (a) or surrounding benign tissue (b). The merged image (right) shows the localization of complement cleavage products within the vasculature (yellow fluorescence) or in its close proximity (green fluorescence). Scale bar, 10 μm. Images are representative of immunofluorescence studies performed on at least 3 wild-type mice. **(c)** Tumor volumes for individual C3-deficient mice (C3-KO) and littermate wild-type controls (C3-WT) measured on various days after tumor cell injection. The last panel (25-26 excised) indicates volumes based on measurements obtained after mice were sacrificed and the tumors removed. Horizontal lines among each group of data points represent the mean tumor volume for that group. The graph is representative of three independent experiments, each with $n = 10$ mice per cohort ($P < 0.0001$ for the entire course of the experiment, two-way ANOVA).
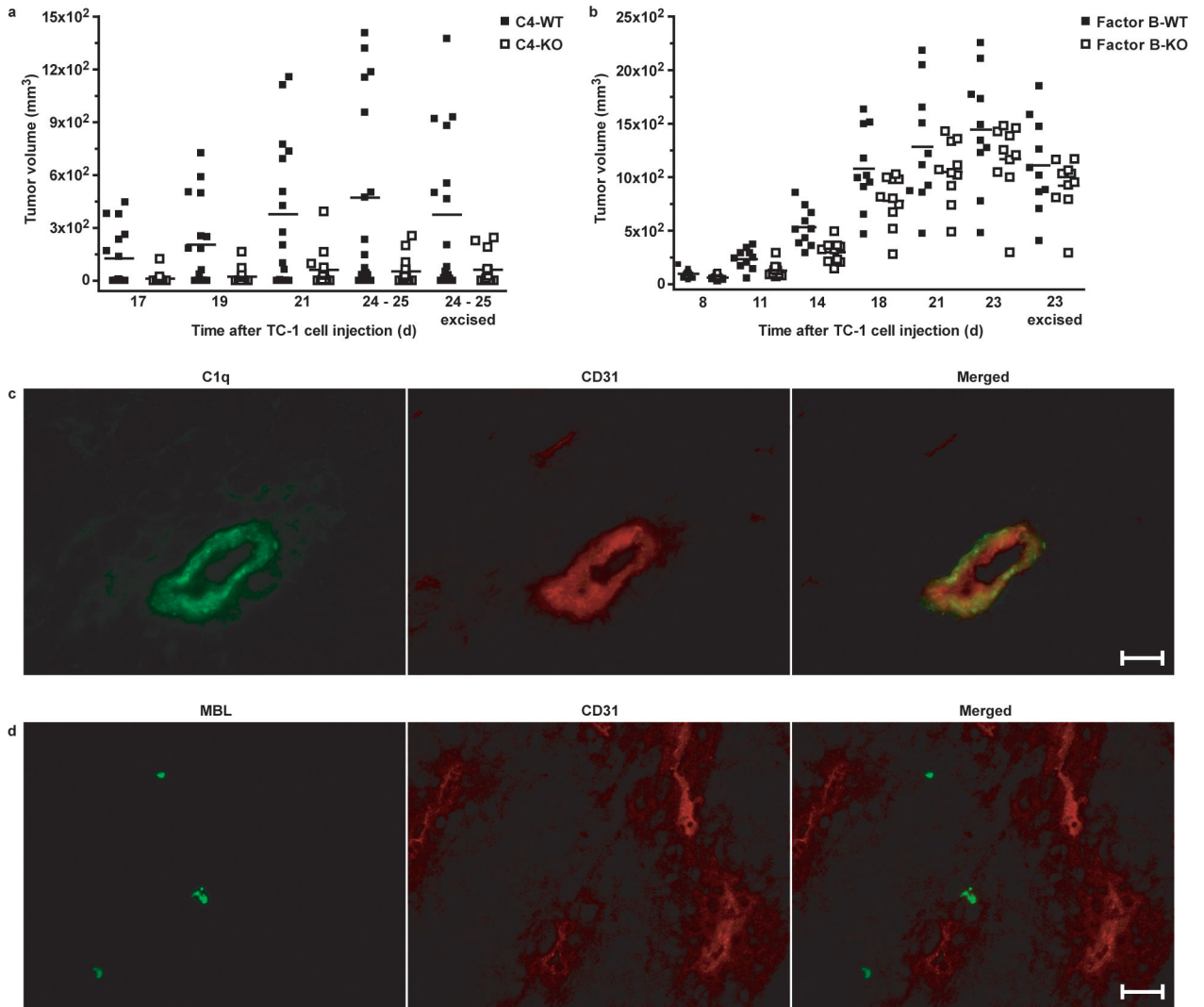
Figure 2.

Involvement of the classical pathway in the activation of complement during tumor growth. **(a)** Tumor volumes for C4-deficient mice (C4-KO) and littermate wild-type controls (C4-WT) measured after tumor cell injection. "24–25 excised" indicates measurements of excised tumors. Horizontal lines represent mean tumor volumes for each group. The graph is representative of two independent experiments, with n_1 14 and $n_2 = 12$ mice per cohort ($P < 0.0001$, two-way ANOVA). **(b)** Tumor volumes, as described in (a), for factor B-deficient mice (Factor B-KO) and littermate wild-type controls (Factor B-WT) ($n = 10$ mice per cohort, $P = 0.6126$, two-way ANOVA). **(c,d)** Immunofluorescent detection of C1q, using C1q antibody (left, green fluorescence), or endothelial cells using CD31 antibody (middle, red fluorescence) in frozen sections of an end-point tumor from a wild-type mouse. The merged image (right) shows localization of C1q within the vasculature (yellow fluorescence). (d) Staining as described in (c) but using MBL antibody (left, green fluorescence) instead of C1q antibody. Colocalization is not observed in the merged image (right). For (c) and (d), images are representative of immunofluorescence studies performed on at least 5 wild-type mice, and scale bar represents 10 μm.
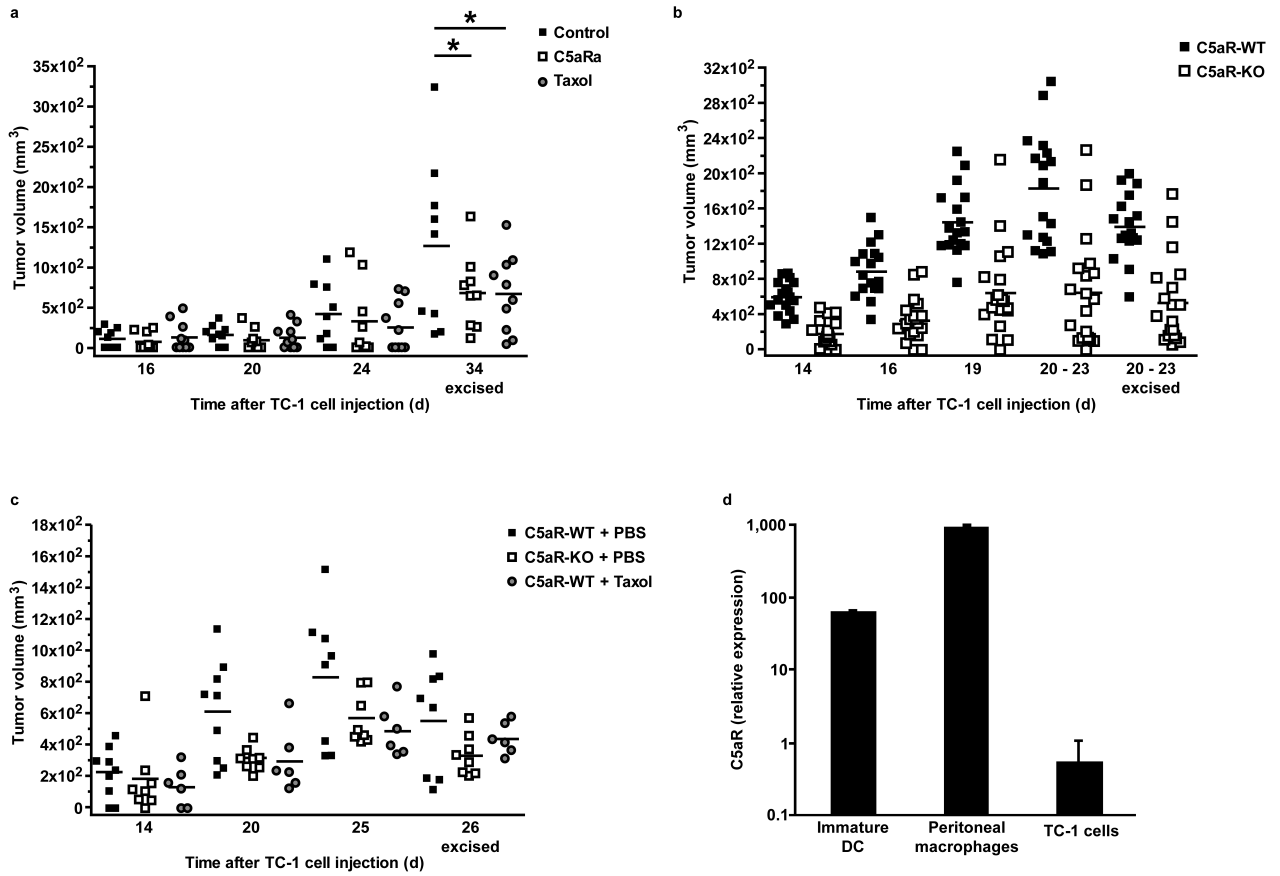
Figure 3.

Lack of C5aR signaling reduces tumor growth with efficiency similar to that of Taxol treatment. **(a)** Tumor volumes for wild-type mice treated with C5aR antagonist (C5aRa), Taxol, or PBS (Control). "34 excised" indicates measurements of excised tumors. Horizontal lines represent mean tumor volumes for each group. The graph is representative for two independent experiments with n_1 9 and $n_2 = 5$ mice per cohort (*, $P < 0.05$, two-way ANOVA, Bonferroni post test). **(b)** Tumor volumes, as described in (a), for C5aR-deficient mice (C5aR-KO) and littermate wild-type controls (C5aR-WT) ($n = 20$ mice per cohort $P < 0.0001$, two-way ANOVA). **(c)** Tumor volumes, as described above, for C5aR-WT mice treated with PBS or Taxol, and C5aR-KO mice treated with PBS (n 6 mice per cohort, $P = 0.004$, two-way ANOVA). **(d)** The relative expression of C5aR in TC-1 cells, immature dendritic cells (DC), and peritoneal macrophages is shown. Data are presented as a ratio of C5aR mRNA to 10^4 GAPDH mRNA molecules. C5aR was considered to be present if more than five copies of mRNA were detected for every 10^4 copies of GAPDH mRNA.
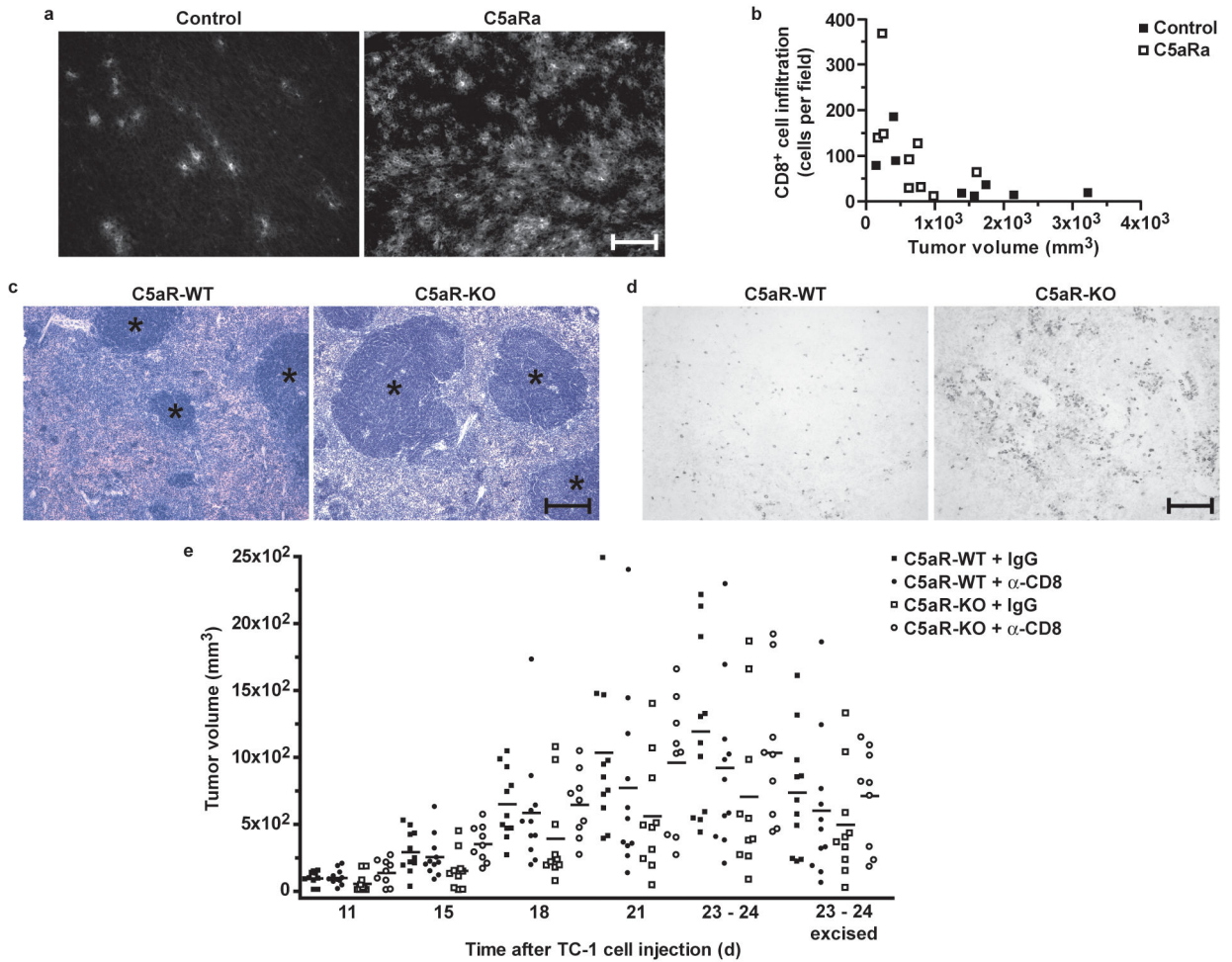
Figure 4.
The anti-tumor T cell response is enhanced in mice lacking C5aR signaling. **(a)** CD8^{+} T cell infiltration of end-point tumor tissue in controls (left) and C5aR antagonist (C5aRa)-treated mice. Fluorescence indicates CD8 expression on infiltrating T cells. Scale bar, 30 μm. **(b)** Number of CD8^{+} T cells infiltrating tumors versus tumor volumes, based on immuofluorescence studies in (a), expressed as cells counted per 200× field (n 8 mice per cohort, $P = 0.0180$, $r = -0.5653$, Pearson correlation). **(c)** Hematoxylin and eosin-stained end-point spleen sections from littermate wild-type (C5aR-WT, left) or C5aR-deficient (C5aR-KO, right) tumor-bearing mice. Asterisks indicate areas of white pulp. **(d)** BrdU-positive end-point splenocytes in C5aR-WT (left) or C5aR-KO (right) mice bearing tumors. For (c) and (d), n 9 mice per cohort; scale bar, 60 μm. **(e)** Tumor volumes for C5aR-KO and C5aR-WT mice treated with either IgG or CD8 antibody (α-CD8). "23-24 excised" indicates measurements of excised tumors. Horizontal lines represent mean tumor volumes for each group (n 9 mice per cohort). Statistically significant differences (two-way ANOVA) were observed between: C5aR-WT + IgG vs. C5aR-KO + IgG ($P = 0.0003$) and C5aR-KO + IgG vs. C5aR-KO + α-CD8 ($P = 0.0006$).
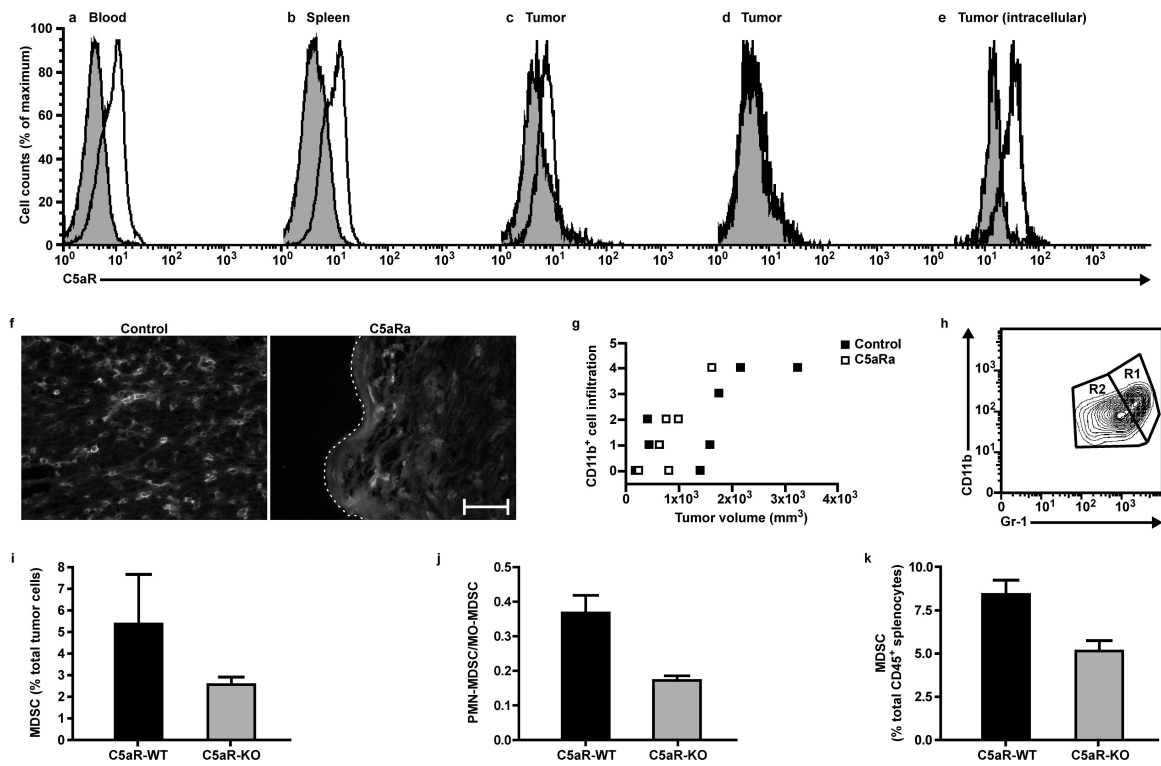
Figure 5.

The migration of myeloid-derived cells into tumors is C5aR dependent. **(a–e)** Expression of C5aR (white areas) versus isotype controls (grey areas) on MDSCs of wild-type mice (n 5) from blood (a), spleen (b) and tumors (c–e). The same cells as shown in (d) were permeabilized before staining (e). **(f)** CD11b$^+$ cell infiltration of tumors from control (left) or C5aR antagonist (C5aRa, right) treated mice. The white dashed line represents the tumor border. Scale bar, 30 μm. **(g)** Quantification of CD11b$^+$ cells infiltrating tumors in relation to tumor volumes, based on (f) (n 6 mice per cohort, $P = 0.0003$, $r = 0.7670$, Pearson correlation). **(h)** Representative contour plot showing characteristics of CD45$^+$CD11b$^+$Gr-1$^+$ cells from tumors from littermate wild-type (C5aR-WT) mice. R1, PMN-MDSCs; R2, MO-MDSCs. **(i)** The percentages of total MDSCs from tumors from C5aR-WT and C5aR-KO mice ($P = 0.23$, t-test). **(j)** Ratio of PMN-MDSCs to MO-MDSCs in the total tumor MDSC population in C5aR-WT and C5aR-KO mice ($P = 0.001$, t-test). **(k)** The percentages of CD11b$^+$Gr-1$^+$ MDSCs from CD45$^+$ splenocytes from C5aR-WT and C5aR-KO mice. ($P = 0.0024$, t-test). For (i)-(k), bars represent mean values + SEM and $n = 16$ mice per cohort.
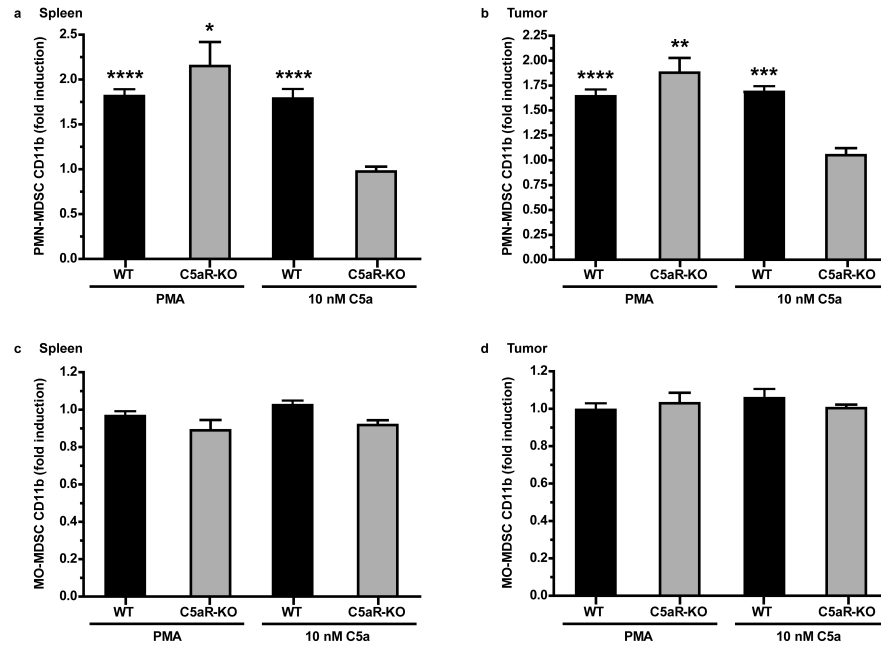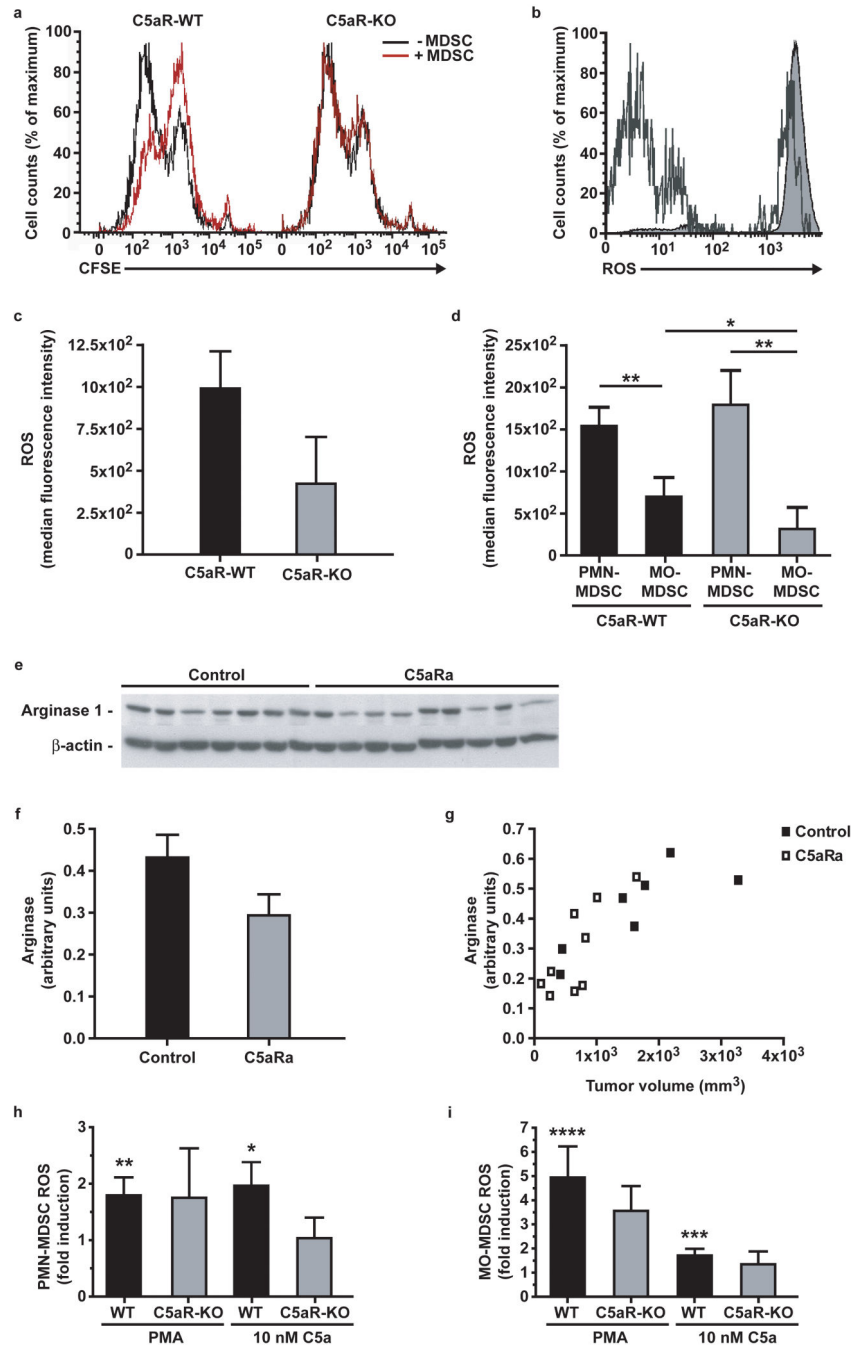
Figure 6.
C5a upregulates CD11b expression in PMN-MDSCs. **(a, b)** Induction of CD11b expression on PMN-MDSCs, as determined by flow cytometry analysis, obtained from the spleens (a) or tumors (b) of wild-type (WT) or C5aR-deficient (C5aR-KO) mice, after treatment with PMA or 10 nM C5a. Graphs show fold increase or decrease in the expression of CD11b in stimulated cells vs. baseline (equal to 1) in unstimulated cells from the same mice (WT or C5aR-KO). **(c, d)** Same analysis as described in (a,b) but for MO-MDSCs. For (a–d), bars represent mean values + SEM (n 5 mice per cohort). The significance of the induction of CD11b expression was determined using one sample t-test (*, $P = 0.0232$; **, $P = 0.0040$; ***, $P = 0.0003$; ****, $P < 0.0001$).

Figure 7.

C5a enhances the suppressive capabilities of tumor associated-MDSCs by regulating ROS and RNS production. **(a)** Inhibition of PHA-induced proliferation of CD3^{+} splenocytes from non-tumor-bearing wild-type mice in the presence of Gr-1^{+} MDSCs from tumors from wild-type (C5aR-WT) or C5aR-deficient (C5aR-KO) mice ($n = 3$ per cohort). **(b)** Representative histogram illustrating ROS and RNS production in MDSCs from tumors from C5aR-WT (grey area) and C5aR-KO (white area) mice. **(c)** Quantification of ROS and RNS production by MDSCs from tumors from C5aR-WT and C5aR-KO mice ($P = 0.0210$, Wilcoxon). **(d)**

Quantification of ROS and RNS production by PMN-MDSCs and MO-MDSCs from tumors of C5aR-WT and C5aR-KO mice (*$P = 0.0342$, ** $P = 0.0005$, Wilcoxon). For (c) and (d), bars represent mean values of median fluorescence + SEM, and n 12 mice per cohort. **(e)** Arginase-1 expression in tumors from control and C5aR antagonist-treated (C5aRa) mice. **(f)** Quantification of immunoblot shown in (e) ($P = 0.0844$, t-test). **(g)** Correlation between arginase-1 expression from (f) and tumor volumes in control and C5aRa-treated mice (Control $P = 0.0256$, $r = 0.8147$ and C5aR $P = 0.0105$, $r = 0.7947$, Pearson correlation). **(h)** Induction of ROS and RNS in PMN-MDSCs, from the spleens of wild-type (C5aR-WT) or C5aR-deficient (C5aR-KO) mice, after treatment with PMA or 10 nM C5a. Graph shows fold increase in ROS and RNS in stimulated cells vs. baseline in unstimulated cells from the same mice. **(i)** Same analysis as described in (h) but for MO-MDSCs. For (h) and (i), bars represent mean values + SEM and n   5 mice per cohort; *, $P = 0.0382$; **, $P = 0.0270$; ***, $P = 0.0245$; ****, $P < 0.0092$, one sample t-test.